ELSEVIER

Contents lists available at ScienceDirect

International Journal of Mass Spectrometry

journal homepage: www.elsevier.com/locate/ijms



Flash pyrolysis mechanism of trimethylchlorosilane

Kuanliang Shao, Jonah Brunson ¹, Yi Tian ², Jingsong Zhang^{*}

Department of Chemistry, University of California, Riverside, CA, 92521, United States



ARTICLE INFO

Article history:
Received 31 March 2022
Received in revised form
31 August 2022
Accepted 5 September 2022
Available online 15 September 2022

Keywords: Mass spectrometry Density functional theory Pyrolysis Trimethylchlorosilane

ABSTRACT

The thermal decomposition mechanism of trimethylchlorosilane at temperatures up to 1400 K was investigated using flash pyrolysis microreactor coupled with vacuum ultraviolet (118.2 nm) photoionization time-of-flight mass spectrometry. The main initiation reaction of the parent molecule was identified to be HCl molecular elimination producing Me₂Si=CH₂, and its onset temperature was estimated to be around 1210 K. The methyl loss channel was also observed at an onset temperature of ~1280 K. Other possible initiation pathways such as chlorine atom loss and methane molecular elimination were considered to be insignificant. Quantum chemistry calculations at the UCCSD(T)/cc-pVTZ// UM05-2X/aug-cc-pVDZ level of theory were performed to study the energetics of the possible initiation pathways. The theoretical calculations revealed that the HCl elimination channel via a van der Waals intermediate was the most energetically favored pathway among all the initiation channels, in agreement with the experimental observations. Transition state theory (TST) and variational transition state theory (VTST) calculations were employed to calculate unimolecular dissociation rate constants of the initiation reactions at elevated temperatures. The results supported the experimental observations and reaction energetics calculations that the HCl molecular elimination reaction was the most prominent initiation reaction and the CH3 loss channel was a significant initiation reaction channel. Secondary reactions of the initial products were identified, and the possible mechanisms were proposed.

© 2022 Elsevier B.V. All rights reserved.

1. Introduction

The preparation of silicon carbide (SiC) by chemical vapor deposition (CVD) is important in industrial processing [1,2]. A series of chloromethylsilanes (SiMe_{4-x}Cl_x) have been considered as suitable CVD precursors [3,4], and it therefore becomes important to understand their gas-phase thermal decomposition behaviors. A number of studies have focused on the pyrolysis mechanisms of several SiMe_{4-x}Cl_x species, such as trichloromethylsilane and dichlorodimethylsilane [3,5–11]. However, there are relatively fewer investigations on the gas-phase thermal decomposition of trimethylchlorosilane. The gas-phase dyotropic arrangement between chloromethyldimethylsilane and trimethylchlorosilane was

studied by Martin et al. using a static cell at 636 K to 690 K [12]. It reported that the isomerization between omethyldimethylsilane and trimethylchlorosilane was carried out in two parallel channels, a concerted dyotropic rearrangement and a free radical chain reaction. Davidson et al. examined the pyrolysis mechanisms of trimethylchlorosilane by using a low-pressure pyrolysis technique at temperatures between 1020 K and 1110 K [13]. The reactions were believed to be initiated by Si-C bond rupture (reaction (1)), and the main product was determined to be methane, which was proposed to be formed by a bimolecular reaction (reaction (2)). The CH₂SiClMe₂ radical produced in reaction (2) could further undergo dissociation reaction leading to the formation of ClMeSi=CH2 and •CH3 (reaction (3)). The significant presence of hydrogen chloride was observed, and molecular elimination of HCl (reaction (4)) was proposed as a possible formation channel [13]. With the significant amount of HCl present in the pyrolysis system, several bimolecular reactions involving HCl were identified (reaction (5) and (6)). Trimethylchlorosilane is known for its extreme sensitivity to moisture. Papanastasiou et al. studied the rate coefficient of the reaction between trimethylchlorosilane and OH radical over the 295–375 K temperature range and showed that trimethylchlorosilane may have a short lifetime in the atmosphere

^{*} Corresponding author. Air Pollution Research Center, University of California, Riverside, CA, 92521, United States.

E-mail address: jingsong.zhang@ucr.edu (J. Zhang).

¹ Summer visiting student from Riverside City College. Current address: Department of Molecular, Cell and Systems Biology, University of California, Riverside, California 92521, United States.

² Summer visiting student from the University of Science and Technology of China. Current address: Department of Chemistry, Stony Brook University, New York, NY 11794, United States.

due to its high sensitivity to moisture and radicals [14].

$$CISiMe_3 \rightarrow \bullet SiCIMe_2 + \bullet Me \tag{1}$$

•Me + ClSiMe₃
$$\rightarrow$$
 •CH₂SiClMe₂ + CH₄ (2)

$$\bullet CH_2SiClMe_2 \rightarrow ClMeSi = CH_2 + \bullet Me$$
 (3)

$$ClSiMe_3 \rightarrow Me_2Si = CH_2 + HCl \tag{4}$$

$$CIMeSi = CH_2 + HCl \rightarrow Me_2SiCl_2$$
 (5)

$$\bullet SiClMe_2 + HCl \rightarrow Me_2SiCl_2 + \bullet H \tag{6}$$

Among the SiMe_{4-x}Cl_x compounds mentioned above [4,6–13,15–18], the pyrolysis mechanism of trimethylchlorosilane was less studied. Furthermore, as discussed by Davidson et al., HCl was always present in the pyrolysis system, but its formation mechanism was not completely clear [13]. Therefore, studying the initiation reactions in the thermal decomposition of trimethylchlorosilane, especially on the formation mechanism of HCl, is informative. We describe here an investigation on the flash pyrolysis mechanism of trimethylchlorosilane using a SiC microreactor coupled with vacuum ultraviolet photoionization time-offlight mass spectrometer (VUV-PI-TOFMS) under predominantly unimolecular reaction conditions. The detection of the early reaction products and reactive intermediates at elevated temperatures provided insights into how the dissociation reaction of trimethylchlorosilane was initiated. Quantum chemistry calculations were also employed to study the energetics of possible initiation channels. The experimental evidence for the HCl molecular elimination channel of trimethylchlorosilane leading to the production of dimethylsilene (Me₂Si=CH₂) and HCl (the HCl elimination channel) was found, and the conclusion was supported by the theoretical calculations. Other important initiation reactions and secondary reactions were also examined. A comprehensive decomposition mechanism of trimethylchlorosilane was developed.

2. Experimental and computational methods

The flash pyrolysis of trimethylchlorosilane was performed in a SiC tubular microreactor that was coupled with a vacuum ultraviolet photoionization mass spectrometer, which has been described in detail previously [19-23]. The trimethylchlorosilane precursor (>99%) was purchased from Sigma Aldrich. Precaution was taken during the sample introduction process as trimethylchlorosilane is extremely sensitive to moisture, and it could lead to the production of hexamethyldisiloxane as a major impurity. The liquid sample of trimethylchlorosilane was taken out by a glass syringe and introduced to a bubbler filled with helium gas in a glove box. The mass spectrum showed that the contamination of hexamethyldisiloxane was negligible. The precursor was diluted to ~3.7% in the helium carrier gas at a total pressure of ~970 torr, and the gas mixture passed through a pulse valve which operated at 10 Hz and subsequently expanded into the heated SiC tubular microreactor where the pyrolysis took place. The SiC microreactor was heated resistively by the electric current that passed through, while its temperature was monitored by a type C thermocouple attached outside to the center of the heated section, which was calibrated to the internal temperature. The temperature within the microreactor was not uniform, which had both axial and radial distributions [24]; the microreactor temperature in this work was referred as the calibrated temperature reading from the attached thermocouple.

The residence time within the SiC microreactor was estimated to be less than 100 µs by Guan et al. [24] According to the model proposed by Zagidullin et al., the average centerline pressure within the heated region was estimated to be around 10 torr, and the centerline pressure at the exit of the SiC microreactor was estimated to be around 6 torr [25]. The reaction conditions in the SiC microreactor have been characterized before [20,24,26]. These studies indicated that because the precursors were in a low concentration (a few %) in the inert buffer gas (helium) at a low total pressure (~10 torr), and also because the residence time was short, unimolecular reactions of the precursors were predominant, while bimolecular reactions and wall reactions were minimized. After exiting the microreactor, the reaction intermediates, products, and unreacted precursors supersonically expanded into a molecular beam in the main vacuum chamber and then entered the ionization region after passing through a skimmer. In the ionization region, the molecular beam was intercepted by 118.2 nm VUV radiation. The 118.2 nm VUV radiation was generated by tripling of the 355 nm Nd:Yag laser output in a xenon cell with a xenon pressure of around 17 torr. The ions, which were produced from the photoionization process, gained their vertical velocity in an electric field and then arrived at the multichannel plate detector where their flight time was measured. The time-of-flight (TOF) spectra were recorded by a digital oscilloscope (Tektronix TDS3032, 300 MHz) after signal averaging over 512 laser shots. The mass spectra were obtained by converting the TOF spectra from flight time to mass to charge ratio (m/z).

Ouantum chemistry calculations were performed in addition to the experimental investigations. The energetics of the reactants. products, and transition states involved in the trimethylchlorosilane pyrolysis were calculated. Density functional theory (DFT) calculations for geometry optimizations and zero-point energies were performed at the UM05-2X/aug-cc-pVDZ level of theory, as it was recommended by Sirianni et al. [27] for the geometry optimizations of bimolecular van der Waals complexes identified in this work. The single-point energy calculations were obtained at the UCCSD(T)/cc-pVTZ level, as similar methods have been widely used in benchmark calculations of silane systems [28]. For the zero-point energy calculations, all the zero-point vibrational frequencies were scaled by a factor of 0.9725 as recommended by Laury et al. [29] to account for overestimations in the vibrational frequency calculations. Transition states in this work were verified by IRC running calculation at the UM05-2X/aug-ccpVDZ level of theory. All the computations in this work were carried out using the Gaussian 16 package [30].

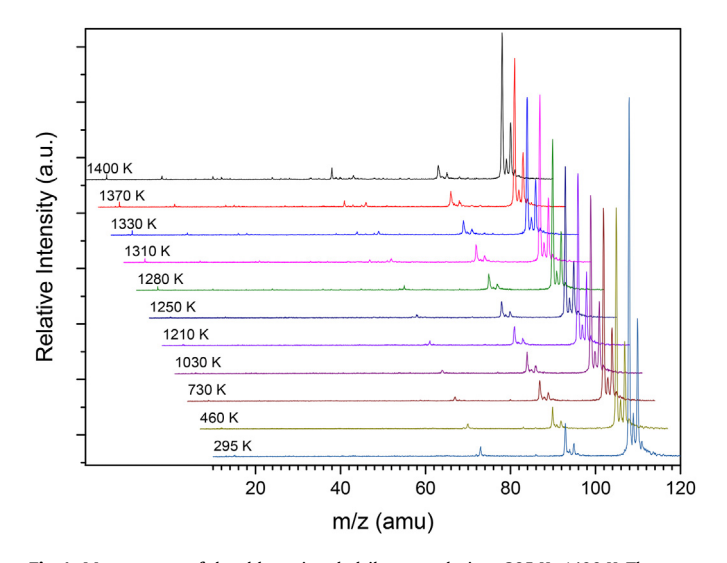
Unimolecular reaction rate constants of the initiation reactions were calculated using transition state theory (TST). For the unimolecular dissociation reaction with a conventional transition state, the rate constant was calculated using TST with Wigner tunneling correction [31–34]. The single point energy and frequencies of reactants and transition states were obtained from DFT calculations at the UM05-2X/aug-cc-pVDZ level of theory using the Gaussian 16 package as described before [30]. For the bond homolysis (barrierless) reactions, variational transition state theory (VTST) with Wigner tunneling correction was applied [31-35]. A series of constrained optimizations along the reaction path were carried out, and at each optimized geometry ("trial transition state"), the potential energy and vibrational frequencies were calculated. The dividing surface for the barrierless reactions at different temperatures were determined by finding the maximum Gibbs free energy change $\Delta G \hbox{\scriptsize o}(T)$ of the "trail transition state" along the reaction pathway at the different temperatures [35]. All the rate constant calculations were performed using the KISTHELP program [33,36,37].

3. Results and discussion

The pyrolysis mass spectra of trimethylchlorosilane at temperatures ranging from 295 K to 1400 K are shown in Fig. 1 and Fig. 2. At 295 K, the m/z = 108, 109, and 110 peaks represented the parent molecule trimethylchlorosilane (ClSiMe₃). The relative natural abundance for ³⁵Cl and ³⁷Cl are 76% and 24%, and the relative abundance for ²⁸Si, ²⁹Si, and ³⁰Si are 92.2%, 4.7%, and 3.1% [38]. The ratio of peak area of m/z = 108 to m/z = 110 is determined to be 2.56 based on Fig. 1, which is close to the theoretical value of 2.86. Other peaks at 295 K, such as m/z = 73, 95, and 97, were caused by photoionization fragmentation of the parent molecule. At 295 K, the signal of m/z = 72 was not caused by photoionization of neutral Me₂Si=CH₂ molecule as the parent molecule could not readily decompose at room temperature. But it was not likely caused by photoionization fragmentation of the parent molecule, as the m/z = 72 signal was not observed in the electron impact spectra of trimethylchlorosilane [39]. The m/z = 72 peak was probably caused by ionization fragments of the very minor parent molecule clusters formed in the molecular beam (which was possible after supersonic cooling of room temperature gas sample). This was consistent with its temperature dependence; when the temperature increased to 460 K, which was not high enough to induce thermal dissociation reactions but sufficient to destroy the molecule clusters in the molecular beam, the m/z = 72 signal disappeared. A very minor peak at m/z = 88 was probably an impurity in the liquid sample, as its signal kept minor and nearly constant throughout all temperatures and could be treated as a spectator at all temperatures.

3.1. The HCl molecular elimination channel forming $Me_2Si = CH_2$

As shown in Figs. 1 and 2, the m/z=72 peak was first observed at 295 K. However, as discussed earlier, it was likely caused by the ionization of molecule clusters in the molecular beam. The signal of the m/z=72 peak reappeared at 1210 K, and its intensity was nearly constant until reaching 1400 K. This indicated that Me₂Si=CH₂ was formed via the HCl elimination channel (reaction (4)) of the parent molecule. The appearance of the m/z=68 peak also served as evidence for the presence of Me₂Si = CH₂, as the SiC₃H₄ species was readily produced by secondary reactions of Me₂Si=CH₂ according to previous studies [19,40]. The counter fragment of the elimination reaction, HCl, was not observed since its ionization potential of



 $\textbf{Fig. 1.} \ \ \text{Mass spectra of the chlorotrimethylsilane pyrolysis at 295 K-1400 K. The mass spectra are offset for clarity. }$

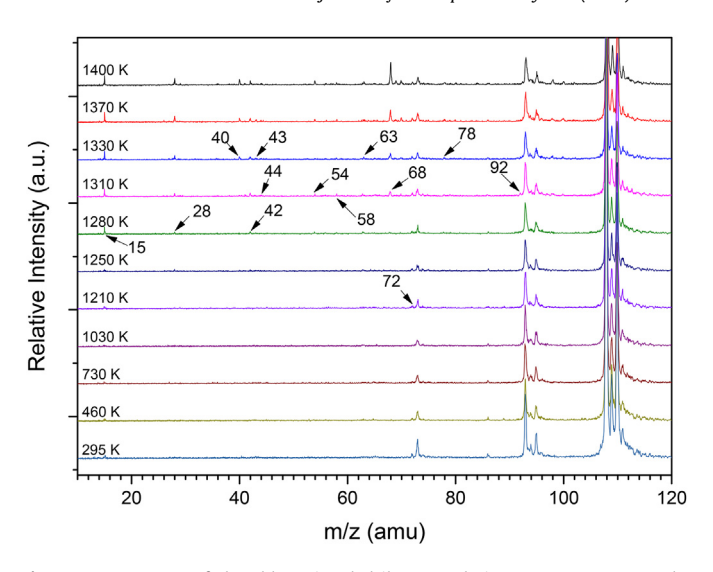


Fig. 2. Mass spectra of the chlorotrimethylsilane pyrolysis at 295 K-1400 K. The spectra were enlarged to identify the peaks of smaller fragments. The mass spectra are offset for clarity.

12.79 eV [41] is higher than the photon energy of the 118 nm (10.49 eV) laser radiation. As will be discussed later, trimethylsilyl radical losing one hydrogen atom forming Me₂Si=CH₂ was considered to be negligible (as the production of Cl and •SiMe₃ from the parent molecule was very small).

Quantum chemistry calculations on the energetics of the initiation reactions of trimethylchlorosilane were summarized in Fig. 3 (more information on the geometries of the species involved is provided in the Supplementary Materials). The HCl molecular elimination channel was determined to have the lowest energy barrier. Trimethylchlorosilane overcomes an energy barrier (TS2) of 75.4 kcal/mol and forms a van der Waals complex at an energy of 71.2 kcal/mol relative to Me₃SiCl. The van der Waals complex may further decompose into Me₂Si=CH₂ and HCl (at an energy of 75.2 kcal/mol). Overall, Me₂Si=CH₂ and HCl can be viewed to be formed via TS2 with a 75.4 kcal/mol energy barrier. Compared to other possible initiation channels, the HCl elimination channel has the lowest energy barrier and is the most energetically favored.

3.2. Other initiation channels

Two other possible initiation channels of the trimethylchlorosilane pyrolysis are the CH₃ loss channel (reaction (1)) and the Cl loss channel (reaction (7)). According to Figs. 1 and 2, the m/ $z = 73 \text{ (•SiMe}_3) \text{ and the } m/z = 93 \text{ (•Si}^{35}\text{ClMe}_2) \text{ and } 95 \text{ (•Si}^{37}\text{ClMe}_2)$ signals appeared as photoionization fragmentation peaks at room temperature. With the increase of temperature, the peak intensities remained nearly constant, suggesting that the thermal decomposition contributions to the signal were trivial. The ratio of peak area for m/z 93/108 and 73/108 (where the parent peak was at m/z108) were plotted in Fig. 4. It shows that the curve remained nearly flat when the temperature increased, and no significant increase of the curve was observed. The m/z = 15 signal for the methyl radical was first observed at 1280 K, which suggested that the onset temperature for reaction (1) was around 1280 K. The onset temperature for reaction (1) was higher than that of reaction (4), indicating that reaction (1) was less significant. Also based on the energetics calculations in Fig. 3, the CH₃ loss channel has an energy threshold of 90.0 kcal/mol, while the threshold energy for the Cl loss channel was determined to be 112.8 kcal/mol; both were much higher than the HCl molecular elimination channel (reaction (4)),

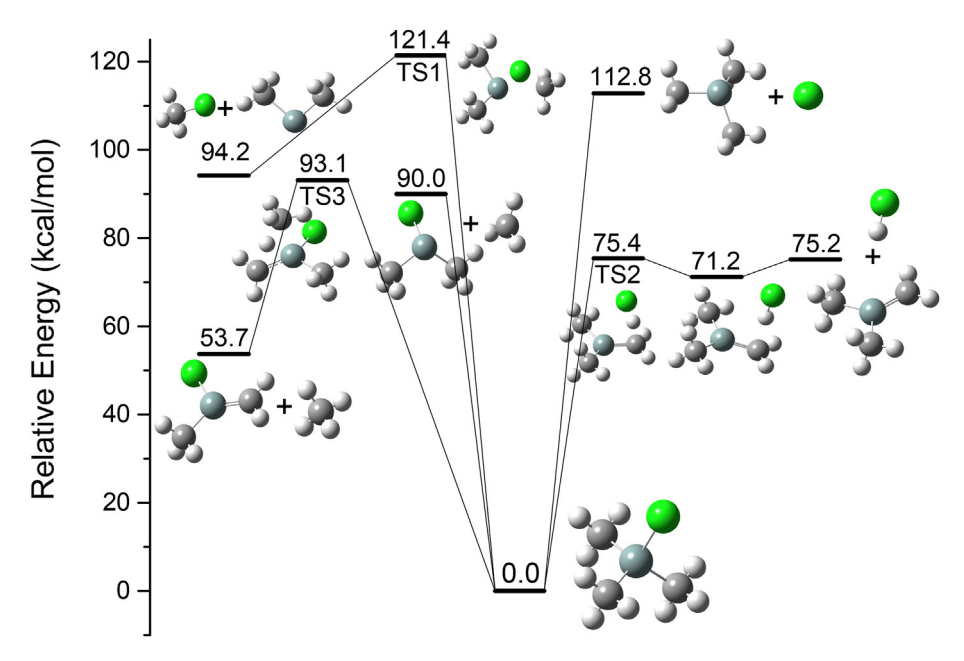


Fig. 3. Energetics (0 K) of the possible initiation channels for the pyrolysis of trimethylchlorosilane at the UCCSD(T)/cc-pVTZ//UM05-2X/aug-cc-pVDZ level.

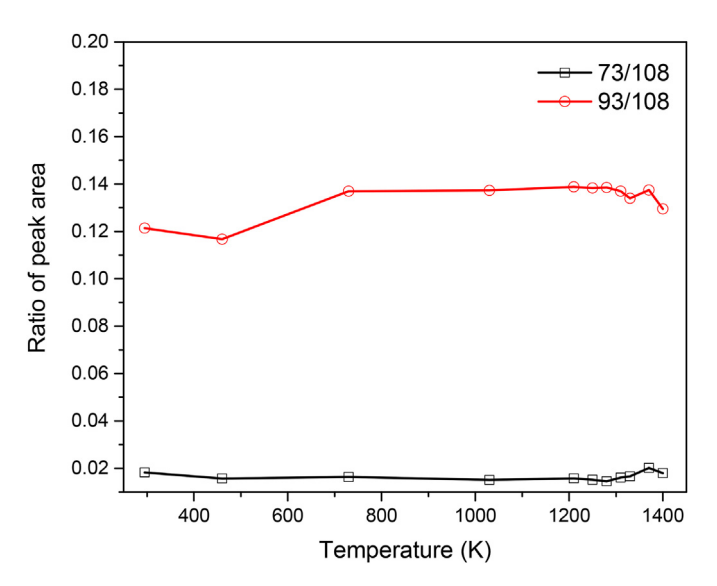


Fig. 4. The plot of the m/z=73 and 93 peak area over m/z=108 peak area in the temperature range from 295 K to 1400 K.

but the CH₃ loss channel (1) was more thermodynamically favored than the Cl loss channel (7).

$$ClSiMe_3 \rightarrow \bullet SiMe_3 + \bullet Cl \tag{7}$$

A very minor peak of m/z = 92 appeared at 1310 K, suggesting the production of ClMeSi=CH₂, and it disappeared as the temperature further increased. ClMeSi=CH₂ was probably formed by the methane elimination reaction of ClSiMe₃ (reaction (8), the CH₄ elimination channel) or the hydrogen loss reaction of •SiClMe₂ (reaction (9)). In Fig. 3, the formation of MeClSi=CH₂ and CH₄ was the most thermodynamically favored pathway with a relative energy of 53.7 kcal/mol, although kinetically the energy barrier via TS3 (93.1 kcal/mol) is still much higher than that of TS2. The CH₄ elimination pathway (reaction (8)) was considered minor because of its higher energy barrier. Similarly, secondary loss of one

hydrogen atom by •SiClMe₂ (produced from reaction (1)) could also lead to the formation of the m/z=92 peak. According to Davidson et al. [13], ClMeSi=CH₂ was formed from secondary dissociations of •CH₂Si(Cl)Me₂ (reaction (3)), which was produced from a series of bimolecular reactions. However, since the signal of •CH₂SiClMe₂ was not detected (Figs. 1 and 2), bimolecular reactions were greatly minimized, and the contribution of reaction (3) to the appearance of the m/z=92 peak and the methyl radical was also considered trivial.

$$ClSiMe_3 \rightarrow MeClSi = CH_2 + CH_4 \tag{8}$$

$$\bullet Si(Cl)Me_2 \rightarrow MeClSi = CH_2 + \bullet H \tag{9}$$

3.3. Unimolecular reaction rate constant calculations for the initiation reactions

The unimolecular reaction rate constants of the abovementioned initiation reactions at different temperatures were calculated using the TST/VTST theory and are summarized in Figs. 5 and 6 (more information on the unimolecular reaction rate constant calculations is provided in the Supplementary Materials). At low temperatures (~1200 K), the HCl elimination channel is the most kinetically favored pathway. As the temperature further increased (above ~1300 K), the CH₃ loss channel started to become significant, while the reaction rate constants for the other three reaction channels remained relatively small. Although there were distributions of temperature in the microreactor, one could still compare the calculated unimolecular reaction rate constants of competing reactions (using the temperature measured in the center region of the microreactor) to determine the relative importance of each reaction. The results of the rate calculations are consistent with the calculated reaction energetics (Fig. 3) and the experimental observations.

As shown in Fig. 6, the calculated rate constant for the HCl elimination channel remained almost constant until around 1050 K and was found to significantly increase at around 1210 K and above. This is consistent with the experimental observation that the signal

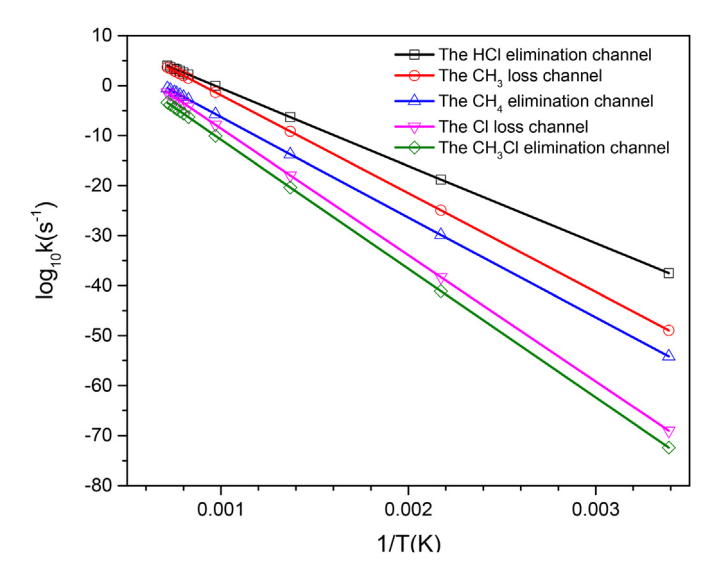


Fig. 5. The unimolecular rate constant calculations of all the initiation reactions with the TST/VTST method. The results are displayed in the form of \log_{10} k vs 1/T.

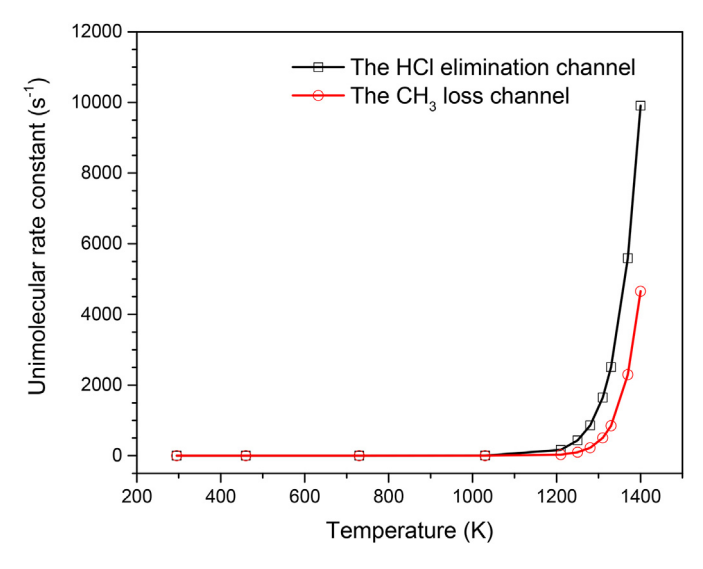


Fig. 6. The unimolecular rate constant calculations of the HCl elimination channel and the ${\rm CH_3}$ loss channel with the TST/VTST method.

of Me₂Si=CH₂ (m/z=72) was first found at around 1210 K. The calculated rate constant for the CH₃ loss channel showed a similar trend at higher temperatures. The rate constant for the CH₃ loss channel increased significantly around 1280 K and kept increasing sharply as the temperature further increased. This is also consistent with the first appearance of the m/z=15 signal at 1280 K, which indicated that the onset temperature of the Si–C bond fission was around 1280 K.

As indicated in Fig. 5, compared to the HCl elimination and CH₃ loss channels, the calculated rate constants for the CH₄ elimination channel, the Cl loss channel, and the CH₃Cl elimination channel were significantly smaller. For example, the rate constant for the CH₄ elimination channel at 1400 K was 0.3 s⁻¹ and that for the Cl loss channel at 1400 K was 0.05 s⁻¹, while the rate constant for the HCl elimination channel at the lower temperature of 1210 K was $165 \, {\rm s}^{-1}$, which is three or more order of magnitude larger. And this is consistent with the experimental observations that the HCl elimination channel and the CH₃ loss channel are more significant

than the other initiation reaction pathways.

3.4. Secondary reactions

Evidence for the occurrences of secondary reactions was also observed and was found to be consistent with the previous experimental and theoretical studies [18,19,23,40]. At 1310 K, the m/z = 68 and 70 peaks were first observed. According to Shao et al. [18] and Liu et al. [40], the SiC₃H₆ and SiC₃H₄ species were produced by sequential dehydrogenation reactions of Me₂Si=CH₂ (reaction (10)-(12)). Liu et al. investigated the energetics of the secondary reactions of Me₂Si=CH₂ in detail at the UB3LYP/ 6-311++G(d,p) level of theory [40]. According to Liu et al., the overall energy barrier of the multistep isomerization channel from Me₂Si=CH₂ to :Si(H)C₃H₇ (reaction (10)) is 62.6 kcal/mol relative to Me₂Si=CH₂. The H₂ elimination of :Si(H)C₃H₇ producing :Si= CHCH₂CH₃ (reaction (11)) was identified as the most energetically favored pathway for the appearance of the m/z = 70 peak, with an energy barrier of 65.4 kcal/mol relative to Me₂Si=CH₂. :Si= CHCH₂CH₃ could further lose an H₂ forming :Si=CHCH=CH₂ (m/ z = 68) with a total threshold energy of 57.9 kcal/mol (reaction (12)). :Si(H)C₃H₇ could also directly dissociate to Si and C₃H₈ (m/ z = 44) with an energy barrier of 58.2 kcal/mol (reaction (13)). This is consistent with the mass spectra in Fig. 2, where the m/z = 44peak first appeared at 1310 K.

$$Me_2Si = CH_2 \rightarrow : Si(H)C_3H_7 \tag{10}$$

$$: Si(H)C_3H_7 \rightarrow : Si = CHCH_2CH_3 + H_2$$
 (11)

$$: Si = CHCH2CH3 \rightarrow : Si = CHCH = CH2 + H2$$
 (12)

$$: Si(H)C_3H_7 \to Si + C_3H_8$$
 (13)

At 1310 K, the signals of m/z = 58, 56, and 54 were detected, which corresponded to :SiMe₂, SiC₂H₄, and SiC₂H₂ respectively. However, these peak intensities were very small. As the temperature further increased, the signal of m/z = 58 and 56 turned trivial, while the signal of m/z = 54 remained nearly constant. The formation of :SiMe2 might be caused by the chlorine loss reaction of SiClMe₂, or the methyl loss reaction of SiMe₃. According to Fig. 4 and the discussions above, the secondary reactions of •SiClMe2 leading to :SiMe₂ were more likely to take place, since reaction (1) was more energetically favored than reaction (7). After the formation of :SiMe2, dehydrogenation reactions started to take place which led to the m/z = 56 peak (reaction (14)) [18,40]. According to Liu et al., the threshold energy for reaction (14) was 56.4 kcal/mol. :Si=CHCH₃ could further lose one H₂ and decompose to :Si=C= CH₂ (reaction (15)). Its threshold energy was calculated to be 44.1 kcal/mol relative to :Si=CHCH₃ [40]. The possible secondary reaction product from the secondary decomposition of SiClMe2 (reaction (16)), :SiClMe (m/z = 78), was first observed at 1330 K, and the signal of m/z = 63 (Si³⁵Cl) was detected at 1330 K, which suggested further secondary reactions of :SiClMe. The isotopic signal of m/z = 65 (Si³⁷Cl) was hardly observed due to its small peak intensity. SiCl could further lose a Cl atom forming Si, although the signal of Si (m/z = 28) could evolve from multiple sources.

$$: SiMe_2 \rightarrow : Si = CHCH_3 + H_2 \tag{14}$$

$$: Si = CHCH_3 \rightarrow : Si = C = CH_2 + H_2$$
 (15)

$$SiClMe_{2} \xrightarrow{-CH_{3}} : SiClMe \xrightarrow{-CH_{3}} SiCl$$
 (16)

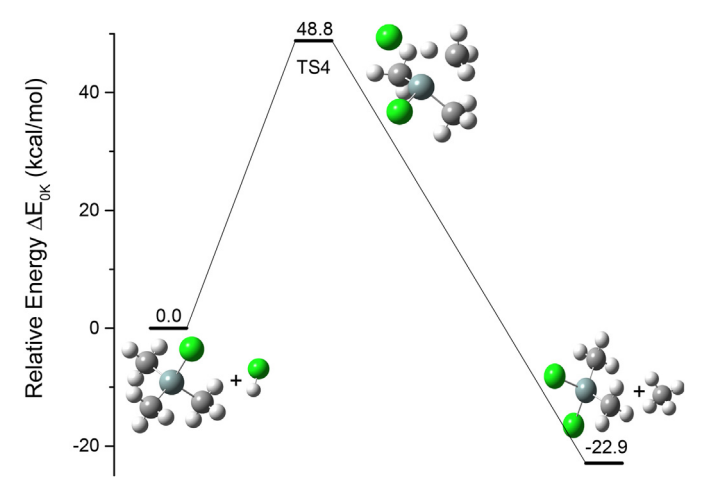


Fig. 7. Energetics (0 K) of the bimolecular reaction between trimethylchlorosilane and HCl at the UCCSD(T)/cc-pVTZ//UM05-2X/aug-cc-pVDZ level.

At 1280 K, the signal of m/z=42 was detected, and when the temperature increased to 1330 K, the m/z=40 peak was observed. The peak m/z=40 and 42 signals remained constant as the temperature increased. The m/z=42 peak corresponds to Si=CH₂ or C₃H₆, and the m/z=40 peak represents SiC. The m/z=42 signal at 1280 K was likely produced by the methane elimination mechanism from :SiMe₂ (reaction (17)) with an energy barrier of 56.6 kcal/mol according to Liu et al. [40]. Alternatively, it could be evolved from the secondary decompositions of :Si=CHCH₂CH₃ (reaction (18)), and this is consistent with the appearance of m/z=28 signal (Si) at 1280 K.

$$: SiMe_2 \xrightarrow{-CH_4} : Si = CH_2$$
 (17)

$$: Si = CHCH2CH3 \rightarrow Si + C3H6$$
 (18)

The appearance of the small m/z = 98, 100, and 102 (:SiCl₂)

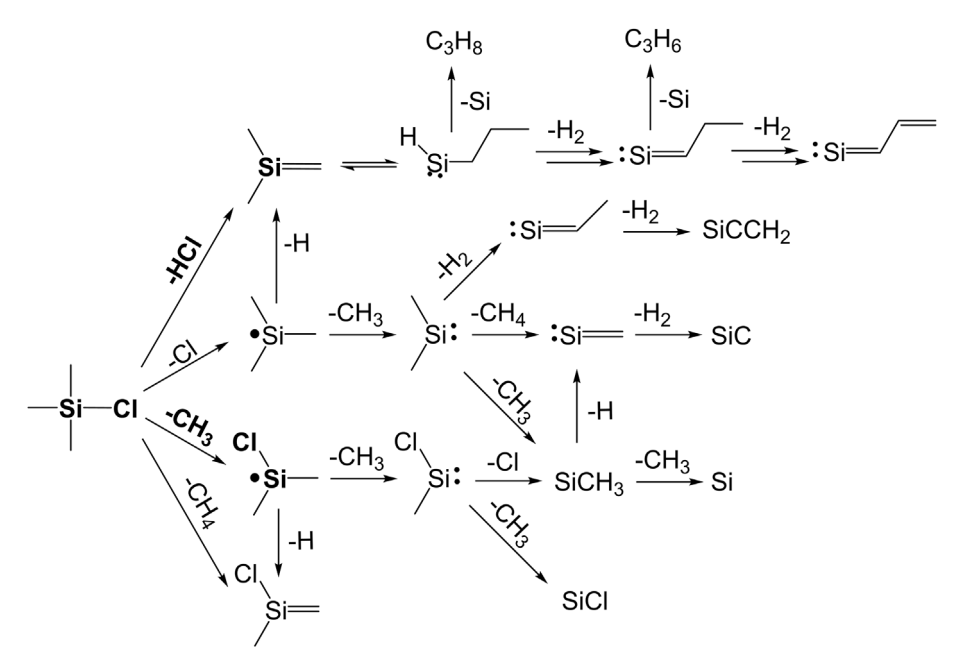
peaks at 1330 K might be associated with some very minor bimolecular reactions at high temperatures between HCl and the parent molecule ClSiMe₃. The HCl, which was produced in abundancy in reaction (4), reacted with ClSiMe₃ and produced Cl₂SiMe₂ (reaction (19)). Then, further decomposition of Cl₂SiMe₂ at high temperatures led to the formation of the SiCl₂ species [6]. In this work, the signal of the SiCl₂ species was much smaller than that in the previous study of the Cl₂SiMe₂ pyrolysis [6], suggesting that the production of Cl₂SiMe₂ and SiCl₂ species were insignificant under the predominantly unimolecular reaction conditions.

$$HCl + ClSiMe_3 \rightarrow Cl_2SiMe_2 + CH_4$$
 (19)

Reaction (19) might need further attention, although it was found insignificant in this work. The quantum chemistry calculations were performed at the UCCSD(T)/cc-pVTZ//UM05–2X/aug-cc-pVDZ level of theory and are displayed in Fig. 7. It shows that reaction (19) is exothermic and has an energy barrier of 48.8 kcal/mol, which indicates that reaction (19) was the most kinetically and thermodynamically favored pathway in this system. This previously ignored reaction pathway might have played an important role in the study by Davidson et al. [13], since it might be another significant bimolecular reaction pathway leading to the major product, methane.

4. Conclusion

The thermolysis of trimethylchlorosilane was studied by flash pyrolysis coupled with molecular beam sampling and VUV-SPI-TOFMS in this work. The quantum chemistry calculations regarding the energetics of several initiation reaction products were performed. The main decomposition mechanism was summarized in Scheme 1. The HCl molecular elimination channel of the parent molecule producing HCl and Me₂Si=CH₂ via a van der Waals intermediate was identified as the predominant pathway. The onset temperature for this reaction was determined to be around 1210 K. The CH₃ loss channel was also observed, and its onset temperature was determined to be around 1280 K. Other possible initiation channels such as the CH₄ elimination channel and the Cl



Scheme 1. The overall decomposition mechanisms of trimethylchlorosilane, which include the initiation reactions and the secondary reactions. The prominent decomposition pathways are marked in bold.

loss channel were less significant. The quantum chemistry calculations and the TST/VTST calculations of the unimolecular reaction rate constants revealed that the HCl elimination channel was the most favorable pathway, which was in consistence with the experimental observations.

Several secondary reaction products have been observed and their formation mechanisms were identified. The secondary reaction of $Me_2Si=CH_2$ leading to the formation of the m/z=70 and m/z=68 signals were also discussed. The secondary reaction products of other species such as $SiMe_2Cl$ or : $SiMe_2$ were also identified. The appearance of the $SiCl_2$ signals at high temperatures was believed to be involved with some minor bimolecular reactions between the main initial product HCl and the parent molecule $ClSiMe_3$.

Author statement

Kuanliang Shao: experimental data acquisition, data analysis, theoretical calculations, writing-original draft preparation, and revisions.

Jonah Brunson: experimental data acquisition and data analysis.

Yi Tian: experimental data acquisition and data analysis.

Jingsong Zhang: project planning, supervision, and writing, reviewing, and editing.

Declaration of competing interest

The authors declare that they have no known competing financial interests or personal relationships that could have appeared to influence the work reported in this paper.

Acknowledgment

This work was supported by the US National Science Foundation (CHE-156636 and CHE-2155232).

Appendix A. Supplementary data

Supplementary data to this article can be found online at https://doi.org/10.1016/j.ijms.2022.116933.

References

- [1] G. Aresta, J. Palmans, M.C.M.v.d. Sanden, M. Creatore, Initiated-chemical vapor deposition of organosilicon layers: monomer adsorption, bulk growth, and process window definition, J. Vac. Sci. Technol. 30 (2012), 041503.
- [2] M.B.J. Wijesundara, R.G. Azevedo, SiC materials and processing technology, in: Silicon Carbide Microsystems for Harsh Environments, Springer New York, New York, NY, 2011, pp. 33–95.
- [3] Y. Funato, N. Sato, Y. Fukushima, H. Sugiura, T. Momose, Y. Shimogaki, Fundamental evaluation of gas-phase elementary reaction models for silicon carbide chemical vapor deposition, ECS Journal of Solid State Science and Technology 6 (2017) P399–P404.
- [4] B.J. Choi, Chemical vapour deposition of silicon carbide by pyrolysis of methylchlorosilanes, J. Mater. Sci. Lett. 16 (1997) 33–36.
- [5] T.M. Besmann, B.W. Sheldon, T.S. Moss III, M.D. Kaster, Depletion effects of silicon carbide deposition from methyltrichlorosilane, J. Am. Ceram. Soc. 75 (1992) 2899–2903.
- [6] J.M. Lemieux, J. Zhang, Letter: thermal decomposition of methyltrichlorosilane, dimethyldichlorosilane and methyldichlorosilane by flash pyrolysis vacuum ultraviolet photoionization time-of-flight nass spectrometry, Eur. J. Mass Spectrom. 20 (2014) 409–417.
- [7] D.E. Cagliostro, S.R. Riccitiello, M.G. Carswell, Analysis of the pyrolysis products of dimethyldichlorosilane in the chemical vapor deposition of silicon carbide in argon, J. Am. Ceram. Soc. 73 (1990) 607–614.
- [8] F. Loumagne, F. Langlais, R. Naslain, Experimental kinetic study of the chemical vapour deposition of SiC-based ceramics from CH₃SiCl₃ H₂ gas precursor, J. Cryst. Growth 155 (1995) 198–204.
- [9] F. Loumagne, F. Langlais, R. Naslain, Reactional mechanisms of the chemical vapour deposition of SiC-based ceramics from CH₃SiCl₃ H₂ gas precursor, J. Cryst. Growth 155 (1995) 205–213.

- [10] G.D. Papasouliotis, S.V. Sotirchos, Experimental study of atmospheric pressure chemical vapor deposition of silicon carbide from methyltrichlorosilane, J. Mater. Res. 14 (2011) 3397—3409.
- [11] S.H. Mousavipour, V. Saheb, S. Ramezani, Kinetics and mechanism of pyrolysis of methyltrichlorosilane, J. Phys. Chem. 108 (2004) 1946–1952.
- [12] J.G. Martin, M.A. Ring, H.E. O'Neal, Gas-phase dyotropic rearrangement of (chloromethyl)dimethylsilane, Organometallics 5 (1986) 1228–1230.
- [13] I.M.T. Davidson, C.E. Dean, Kinetics and mechanism of pyrolysis of some methylchlorosilanes, Organometallics 6 (1987) 966–969.
- [14] D.K. Papanastasiou, F. Bernard, J.B. Burkholder, Trimethylchlorosilane, (CH₃)₃SiCl: OH reaction kinetics and infrared spectrum, Int. J. Chem. Kinet. 52 (2020) 221–226.
- [15] Y. Ge, M.S. Gordon, F. Battaglia, R.O. Fox, Theoretical study of the pyrolysis of methyltrichlorosilane in the gas phase. 3. Reaction rate constant calculations, J. Phys. Chem. 114 (2010) 2384–2392.
- [16] Y. Ge, M.S. Gordon, F. Battaglia, R.O. Fox, Theoretical study of the pyrolysis of methyltrichlorosilane in the gas phase. 1. Thermodynamics, J. Phys. Chem. 111 (2007) 1462–1474.
- [17] Y. Ge, M.S. Gordon, F. Battaglia, R.O. Fox, Theoretical study of the pyrolysis of methyltrichlorosilane in the gas phase. 2. Reaction paths and transition states, I. Phys. Chem. 111 (2007) 1475—1486.
- [18] K. Shao, Y. Tian, J. Zhang, Thermal decomposition mechanism of allyltrichlorosilane and allyltrimethylsilane, Int. J. Mass Spectrom. 460 (2021) 116476–116484.
- [19] X. Liu, J. Zhang, A. Vazquez, D. Wang, S. Li, Mechanistic study of thermal decomposition of hexamethyldisilane by flash pyrolysis vacuum ultraviolet photoionization time-of-flight mass spectrometry and density functional theory. J. Phys. Chem. 123 (2019) 10520–10528.
- [20] P.J. Jones, B. Riser, J. Zhang, Flash pyrolysis of t-butyl hydroperoxide and di-t-butyl peroxide: evidence of roaming in the decomposition of organic hydroperoxides, J. Phys. Chem. 121 (2017) 7846–7853.
- [21] S.D. Chambreau, J. Zhang, J.C. Traeger, T.H. Morton, Photoionization of methyl t-butyl ether (MTBE) and t-octyl methyl ether (TOME) and analysis of their pyrolyses by supersonic jet/photoionization mass spectrometry, Int. J. Mass Spectrom. 199 (2000) 17–27.
- [22] D.W. Kohn, H. Clauberg, P. Chen, Flash pyrolysis nozzle for generation of radicals in a supersonic jet expansion, Rev. Sci. Instrum. 63 (1992) 4003–4005
- [23] K. Shao, Y. Tian, J. Zhang, A mechanistic study of thermal decomposition of 1,1,2,2-tetramethyldisilane using vacuum ultraviolet photoionization time-offlight mass spectrometry, J. Phys. Chem. 126 (2022) 1085–1093.
- [24] Q. Guan, K.N. Urness, T.K. Ormond, D.E. David, G. Barney Ellison, J.W. Daily, The properties of a micro-reactor for the study of the unimolecular decomposition of large molecules, Int. Rev. Phys. Chem. 33 (2014) 447–487.
- [25] M.V. Zagidullin, R.I. Kaiser, D.P. Porfiriev, I.P. Zavershinskiy, M. Ahmed, V.N. Azyazov, A.M. Mebel, Functional relationships between kinetic, flow, and geometrical parameters in a high-temperature chemical microreactor, J. Phys. Chem. 122 (2018) 8819–8827.
- [26] K.H. Weber, J.M. Lemieux, J. Zhang, Flash pyrolysis of ethyl, n-propyl, and isopropyl iodides as monitored by supersonic expansion vacuum ultraviolet photoionization time-of-flight mass spectrometry, J. Phys. Chem. 113 (2009) 583-591.
- [27] D.A. Sirianni, A. Alenaizan, D.L. Cheney, C.D. Sherrill, Assessment of density functional methods for geometry optimization of bimolecular van der Waals complexes, J. Chem. Theor. Comput. 14 (2018) 3004–3013.
- [28] M. Cypryk, B. Gostyński, Computational benchmark for calculation of silane and siloxane thermochemistry, J. Mol. Model. 22 (2016) 35.
- [29] M.L. Laury, S.E. Boesch, I. Haken, P. Sinha, R.A. Wheeler, A.K. Wilson, Harmonic vibrational frequencies: scale factors for pure, hybrid, hybrid meta, and double-hybrid functionals in conjunction with correlation consistent basis sets, J. Comput. Chem. 32 (2011) 2339–2347.
- [30] M.J. Frisch, G.W. Trucks, H.B. Schlegel, G.E. Scuseria, M.A. Robb, J.R. Cheeseman, G. Scalmani, V. Barone, G.A. Petersson, H. Nakatsuji, X. Li, M. Caricato, A.V. Marenich, J. Bloino, B.G. Janesko, R. Gomperts, B. Mennucci, H.P. Hratchian, J.V. Ortiz, A.F. Izmaylov, J.L. Sonnenberg, Williams, F. Ding, F. Lipparini, F. Egidi, J. Goings, B. Peng, A. Petrone, T. Henderson, D. Ranasinghe, V.G. Zakrzewski, J. Gao, N. Rega, G. Zheng, W. Liang, M. Hada, M. Ehara, K. Toyota, R. Fukuda, J. Hasegawa, M. Ishida, T. Nakajima, Y. Honda, O. Kitao, H. Nakai, T. Vreven, K. Throssell, J.A. Montgomery Jr., J.E. Peralta, F. Ogliaro, M.J. Bearpark, J.J. Heyd, E.N. Brothers, K.N. Kudin, V.N. Staroverov, T.A. Keith, R. Kobayashi, J. Normand, K. Raghavachari, A.P. Rendell, J.C. Burant, S.S. Iyengar, J. Tomasi, M. Cossi, J.M. Millam, M. Klene, C. Adamo, R. Cammi, J.W. Ochterski, R.L. Martin, K. Morokuma, O. Farkas, J.B. Foresman, D.J. Fox, Gaussian 16 Rev. C.01, 2016. Wallingford, CT.
- [31] D.G. Truhlar, B.C. Garrett, S.J. Klippenstein, Current status of transition-state theory, J. Phys. Chem. 100 (1996) 12771–12800.
- [32] E. Wigner, The transition state method, Trans. Faraday Soc. 34 (1938) 29–41.
- [33] S. Canneaux, F. Bohr, E. Henon, KiSThelP: a program to predict thermodynamic properties and rate constants from quantum chemistry results, J. Comput. Chem. 35 (2014) 82–93.
- [34] A.W. Jasper, J.A. Miller, S.J. Klippenstein, Collision efficiency of water in the unimolecular reaction CH₄ (+H₂O) ⇒ CH₃ + H (+H₂O): one-dimensional and two-dimensional solutions of the low-pressure-limit master equation, J. Phys. Chem. 117 (2013) 12243—12255.
- [35] M.A. Ali, Computational studies on the gas phase reaction of methylenimine

- (CH₂NH) with water molecules, Sci. Rep. 10 (2020), 10995. [36] S. Mohandas, R.O. Ramabhadran, S.S. Kumar, Theoretical investigation of a vital step in the gas-phase formation of interstellar ammonia $NH_2^+ + H_2 \rightarrow$ NH[±]₃ + H, J. Phys. Chem. 124 (2020) 8373–8382.
- [37] S. Begum, R. Subramanian, Theoretical studies on gas-phase kinetics and mechanism of H-abstraction reaction from methanol by ClO and BrO radicals, RSC Adv. 5 (2015) 39110-39121.
- [38] J. Meija, B. Coplen Tyler, M. Berglund, A. Brand Willi, P. De Bièvre, M. Gröning, E. Holden Norman, J. Irrgeher, D. Loss Robert, T. Walczyk, T. Prohaska, Atomic weights of the elements 2013 (IUPAC technical report), pac 88 (2016)
- [39] W.E.W. Nist, Mass spectrometry data center, director, mass spectra, in: P.J. Linstrom, W.G. Mallard (Eds.), NIST Chemistry WebBook, NIST Standard Reference Database Number 69, National Institute of Standards and Technology, Gaithersburg MD, 2020, https://doi.org/10.18434/T4D303, 20899(retrieved November 2, 2020).
- [40] X. Liu, J. Zhang, A. Vazquez, D. Wang, S. Li, Mechanism of the thermal decomposition of tetramethylsilane: a flash pyrolysis vacuum ultraviolet photoionization time-of-flight mass spectrometry and density functional theory study, Phys. Chem. Chem. Phys. 20 (2018) 18782–18789.
- [41] R.G. Wang, M.A. Dillon, D. Spence, Electron spectroscopy of hydrogen chloride from 5 to 19 eV, J. Chem. Phys. 80 (1984) 63–69.